RBFL 6.0 WORKING WHITE PAPER

RBFL 3D Sine-Intersection Field Mechanics

A volumetric coherence interpretation of phase projection, scaling, and apparent matter clumping

Non-changing core statement

The current 3D RBFL acceleration law is not modified. The sine-intersection mechanism is presented as an explanatory layer for the existing coherence factor $C_\Phi(\mathbf{r}, t)$, not as a new force term.

The law is unchanged; sine-intersection behavior explains the coherence factor

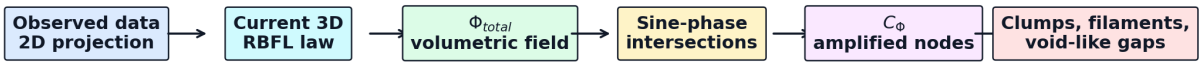

No new force term is added. The mechanism is an explanatory layer for the existing $C_\Phi(\mathbf{r}, t)$.

Theoretical white paper - manuscript-ready draft

June 17, 2026

Prepared for the RBFL 3D-first framework

Abstract

This white paper formalizes the 3D sine-intersection interpretation of RBFL while keeping the present 3D acceleration law unchanged. The central claim is narrow: two-dimensional RBFL representations were appropriate as observed-data diagnostics, because galaxy images, projected density maps, lensing maps, and rotation-curve displays are lower-dimensional measurements. They were not the physical final form. The physical interpretation is now explicitly volumetric.

In the 3D interpretation, baryonic matter anchors local phase-compression volumes inside a saturated parent field. These volumes overlap in ordinary three-dimensional space. Sine-like phase behavior then gives a simple mechanism for local field behavior: constructive intersections produce amplified coherence nodes, while destructive intersections produce suppressed or cancelled response regions. The coherence factor $C_\Phi(\mathbf{r}, t)$ is therefore interpreted as the local volumetric phase-interference response of the baryonic field environment.

This interpretation supplies a defensible explanation for scaling and for apparently random matter clumping. Clumps need not be fundamentally random; they may be projected signatures of stable amplified 3D coherence nodes. Voids or gaps need not be pushed-out matter; they may correspond to regions where amplified coherence fails to form or is locally suppressed. The result is a compact mechanism: observed 2D projection → 3D volumetric law → sine-phase intersections → amplified nodes → scaling, clumps, filaments, gaps, and dark-matter-like morphology.

Keywords: RBFL; 3D phase field; volumetric coherence; sine intersection; wave interference; baryonic anchors; matter clumping; cosmic web; scaling; rotation curves.

Contents

1 Scope and locked constraints

This document is intentionally a mechanism paper, not a general cosmology review. It does not attempt to prove the entire RBFL framework. It explains how the existing RBFL coherence factor may be physically interpreted in 3D as the result of sine-like phase intersection.

Locked position

The 3D RBFL law remains:

$$\boxed{\mathbf{g}_{\mathrm{RBFL}}(\mathbf{r},t) = \mathbf{g}_b(\mathbf{r},t) + C_\Phi(\mathbf{r},t)\sqrt{a_\Phi|\mathbf{g}_b(\mathbf{r},t)|}\,\hat{\mathbf{g}}_b} \tag{1}$$

where

$$\hat{\mathbf{g}}_b = \frac{\mathbf{g}_b}{|\mathbf{g}_b|}. \tag{2}$$

The sine-intersection mechanism does not add a term to Eq. (1). It explains the physical meaning of $C_\Phi(\mathbf{r},t)$.

1.1 Definitions used throughout

Symbol	Meaning	Status
$\mathbf{r} = (x,y,z)$	Three-dimensional spatial position.	Locked 3D coordinate
t	Time coordinate for evolving field states.	Locked
$\mathbf{g}_b$	Baryonic acceleration field from ordinary visible/known baryonic matter.	Locked
$\mathbf{g}_{\mathrm{RBFL}}$	RBFL total acceleration field.	Locked
a_Φ	Universal phase-saturation acceleration scale.	Locked parameter
$C_\Phi(\mathbf{r},t)$	Local coherence response factor. In this paper, interpreted as local volumetric phase-interference response.	Interpretation of existing term
$\Phi_i(\mathbf{r},t)$	Phase response associated with baryonic anchor i.	Mechanism-level model
$\Phi_{\mathrm{total}}(\mathbf{r},t)$	Total 3D phase environment.	Mechanism-level model
$\rho_b(\mathbf{r},t)$	Baryonic matter density.	Observable / model input

Table 1: Minimal notation. The distinction between locked law and mechanism-level interpretation is maintained throughout.

Plain picture

Imagine a room full of invisible ripples, not a flat pond. At some places, ripple peaks meet ripple peaks and make a strong spot. At other places, peaks meet troughs and the ripples fade. RBFL calls the strong stable spots amplified coherence nodes. Matter is expected to organize more easily around those strong spots.

2 Why 2D was used first: observed data are projected data

The reason for earlier 2D or scalar RBFL treatments was observational, not physical. Astronomical data often arrive as projected maps or radial summaries. A galaxy image is a sky-plane projection. A rotation curve is commonly displayed as a speed-versus-radius diagnostic. A lensing reconstruction is a projected surface-potential or convergence map. Public rotation-curve data sets such as SPARC organize disk-galaxy observations into radial and mass-model diagnostics, making them natural first tests for empirical acceleration laws [1].

The earlier scalar form can be written schematically as

$$\boxed{g_{\mathrm{RBFL}}(R) = g_b(R) + C_\Phi(R)\sqrt{a_\Phi g_b(R)}} \tag{3}$$

where R is an observed or modeled radial coordinate. Eq. (3) is a projection-level diagnostic. It is useful because the data are frequently reduced into lower-dimensional profiles.

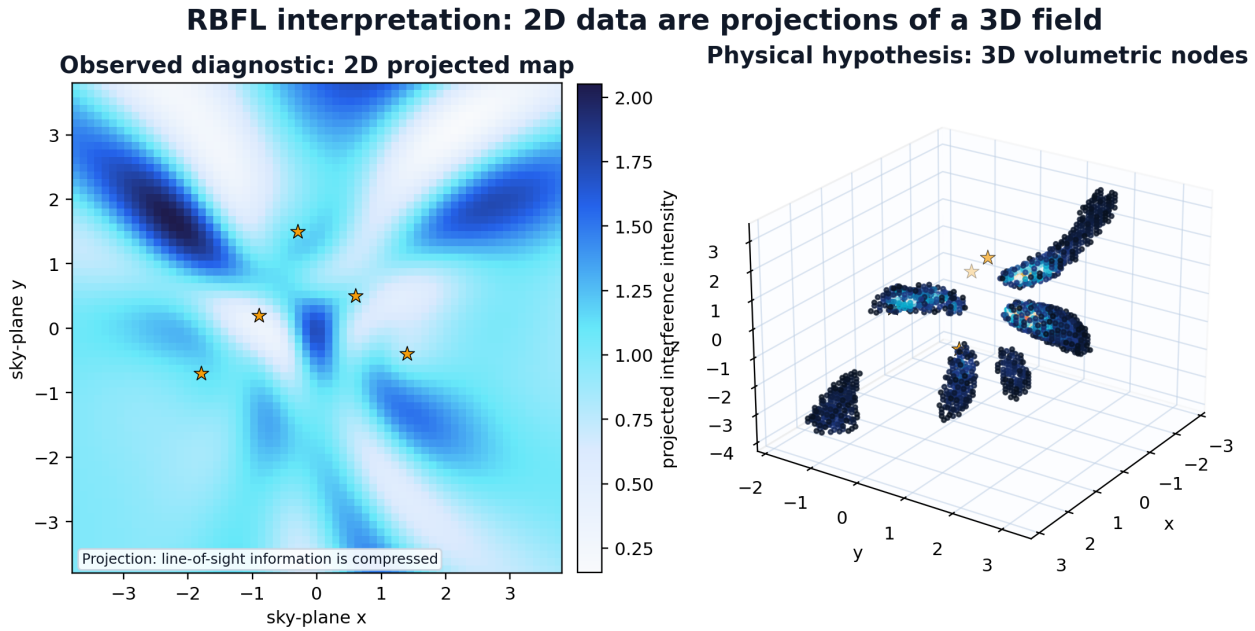

Figure 1: The observed map is a 2D diagnostic. The physical RBFL interpretation is a 3D volumetric field. The left panel compresses line-of-sight structure; the right panel shows how amplified 3D nodes can be hidden by projection.

Reason for 2D

2D was the measurement language. It was not the final field ontology. It allowed RBFL to fit and compare projected observables before the physical interpretation was lifted into a 3D volumetric law.

This distinction protects the published and working forms of RBFL. A 2D or radial plot is not obsolete as a plot. It is obsolete only as a claim about the true dimensional structure of the field. From here forward, any 1D or 2D expression should be read as a projection, slice, visualization, or diagnostic of an underlying 3D field.

3 Why the conversion to 3D is required

A gravitational or phase-field response cannot be fully physical if it only exists on a drawing surface. Baryonic matter occupies volume. Acceleration has direction. Phase overlap occurs through volume. Therefore the correct RBFL object must be defined over $\mathbf{r} = (x, y, z)$, not only over a radius R or a sky-plane coordinate (x, y).

The 3D RBFL law is Eq. (1). The related field environment is written as

$$\boxed{\Phi_{\mathrm{total}}(\mathbf{r}, t) = \Phi_{\mathrm{parent}}(\mathbf{r}, t) + \sum_i \Phi_i(\mathbf{r}, t)} \tag{4}$$

where Φ_{parent} is the saturated parent field and each Φ_i is a baryonic phase contribution.

3D conversion statement

The 3D conversion does not say earlier 2D fits were wrong. It says they were projected measurements of a volumetric field. The law becomes vectorial; the mechanism becomes volumetric; the observations remain projected.

A general observed quantity can be written as a projection operator acting on the 3D field:

$$\boxed{\mathcal{O}_{\rm obs} = \mathcal{P}[\Phi_{\rm total}(\mathbf{r},t), \mathbf{g}_{\rm RBFL}(\mathbf{r},t), \rho_b(\mathbf{r},t)]} \tag{5}$$

where $\mathcal{P}$ represents the observational channel: line-of-sight integration, radial binning, disk-plane extraction, lensing projection, or time-domain residual extraction.

This is the phrase that ties the transition together:

$$\boxed{\text{projection-random does not mean field-random.}} \tag{6}$$

A clump that looks random in a 2D image may be a natural node in 3D.

4 The sine-intersection mechanism

4.1 A baryonic anchor as a phase source

In this mechanism, baryonic matter is treated as a phase-compression anchor. A schematic local phase response from anchor i is

$$\boxed{\Phi_i(\mathbf{r},t) = A_i(\mathbf{r},t)\sin(\mathbf{k}_i\cdot\mathbf{r} - \omega_i t + \theta_i)} \tag{7}$$

where A_i is local amplitude, $\mathbf{k}_i$ is a 3D wave-vector, ω_i is angular frequency, and θ_i is phase offset.

Eq. (7) should be read as a mechanism-level representation, not as a final closed field equation. It says the local baryonic field has a phase state, and phase states can align or oppose one another.

4.2 Constructive and destructive intersection

For two phase components with phases ψ_1 and ψ_2, define

$$\Delta\psi = \psi_1 - \psi_2. \tag{8}$$

A standard interference envelope is

$$\boxed{I_{12} = A_1^2 + A_2^2 + 2A_1A_2\cos(\Delta\psi)} \tag{9}$$

so that

$$\Delta\psi \approx 0 \quad \Rightarrow \quad I_{12} \text{ is amplified,} \tag{10}$$

$$\Delta\psi \approx \pi \quad \Rightarrow \quad I_{12} \text{ is suppressed or cancelled.} \tag{11}$$

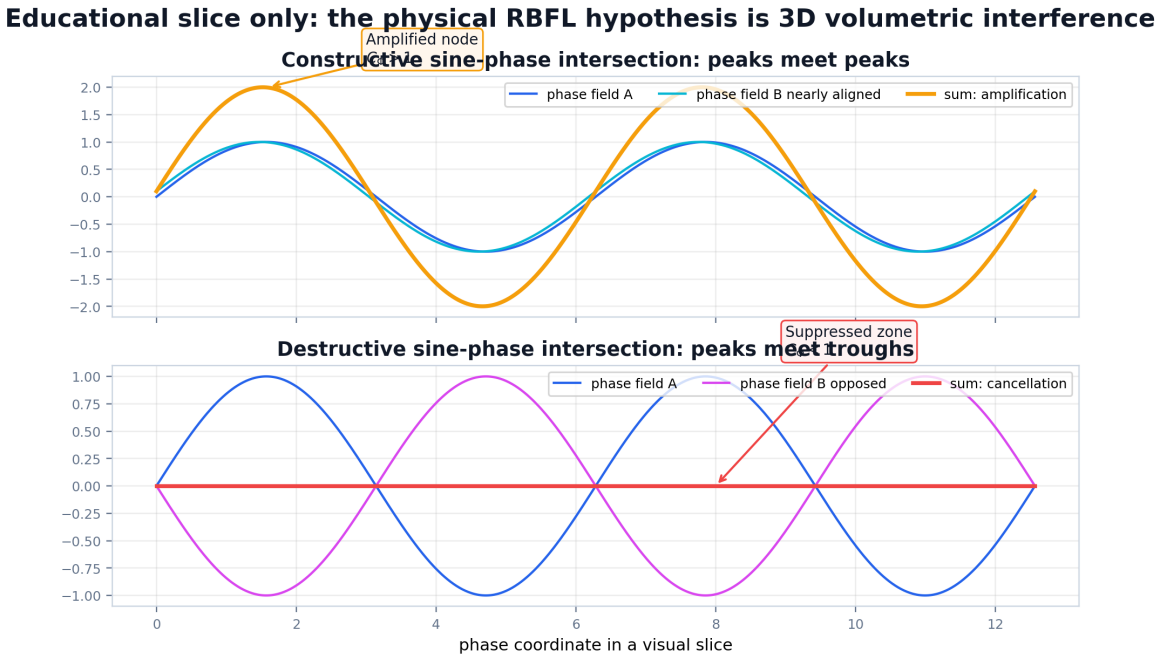

Figure 2: A visual slice of sine-phase behavior. This figure is not the physical dimensional claim; it is the easiest way to see the rule. Constructive alignment produces amplification. Destructive alignment produces suppression or cancellation.

For many anchors, a compact phasor-style interference index can be written as

$$\boxed{\mathcal{I}_\Phi(\mathbf{r},t) = \frac{\left|\sum_i A_i(\mathbf{r},t)e^{i\psi_i(\mathbf{r},t)}\right|^2}{\sum_i A_i^2(\mathbf{r},t) + \varepsilon}} \tag{12}$$

where $\varepsilon > 0$ prevents division by zero. $\mathcal{I}_\Phi$ is not introduced as a new force. It is a possible diagnostic for the local interference intensity that can inform C_Φ.

The coherence factor is then interpreted as a bounded response functional:

$$\boxed{C_\Phi(\mathbf{r},t) = \mathcal{C}[\mathcal{I}_\Phi, \nabla\mathcal{I}_\Phi, \partial_t\mathcal{I}_\Phi, \rho_b, \mathcal{G}]} \tag{13}$$

where $\mathcal{G}$ denotes local geometry, boundary conditions, rotation state, and environmental structure. Eq. (13) is deliberately written as a functional rather than a fixed formula. This keeps the law unchanged while defining what must be modeled and tested.

4.3 Coherence is at amplification points

The most important refinement is that coherence is not generic overlap. Coherence means stable constructive phase alignment.

$$\begin{array}{lcl} C_\Phi(\mathbf{r},t) > 1 & \Rightarrow & \text{amplified coherent node,} \\ C_\Phi(\mathbf{r},t) \approx 1 & \Rightarrow & \text{normal saturated response,} \\ C_\Phi(\mathbf{r},t) < 1 & \Rightarrow & \text{suppressed, cancelled, or incoherent region.} \end{array} \tag{14}$$

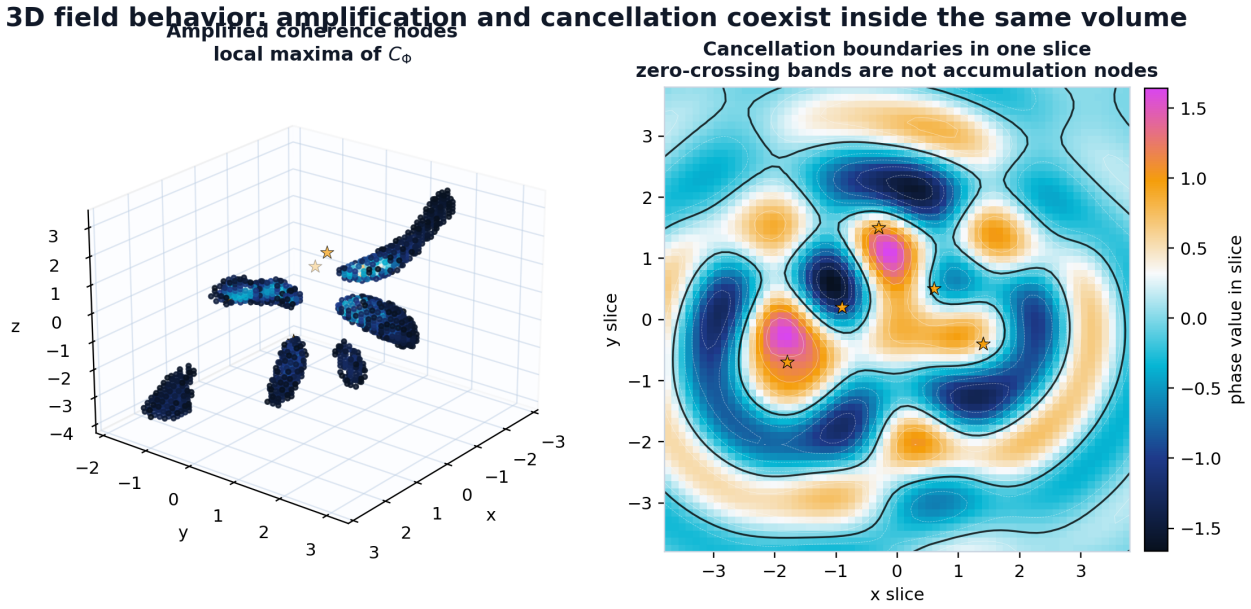

Figure 3: Amplification and cancellation are simultaneous 3D field behaviors. The left panel shows amplified node regions. The right panel is a slice showing cancellation boundaries. A cancellation boundary is not a matter-selection site; it is where phase response is suppressed.

Easy picture

Overlap alone is not enough. Two ripples can meet and grow, or they can meet and disappear. RBFL coherence means the "grow" case: a stable amplified point, line, shell, or volume where the field response is stronger.

5 Field behavior in 3D

The 3D field has three practical classes of behavior.

5.1 Amplified coherence nodes

A stable amplified node is a local maximum of C_Φ. A candidate mathematical condition is

$$\boxed{C_\Phi(\mathbf{r},t) > 1, \qquad \nabla C_\Phi(\mathbf{r},t) = 0, \qquad H[C_\Phi](\mathbf{r},t) \prec 0, \qquad \partial_t C_\Phi \approx 0} \tag{15}$$

where $H[C_\Phi]$ is the Hessian matrix of second derivatives. In plain terms, the node is high, locally peaked, and stable long enough to matter dynamically.

5.2 Normal saturated response

Regions with $C_\Phi \approx 1$ follow the baseline RBFL saturated response. These regions are neither strongly amplified nor strongly cancelled. They are the reference state against which excess or suppression is measured.

5.3 Suppressed or cancelled regions

Regions with $C_\Phi < 1$ are not necessarily regions where matter is actively pushed away. In the RBFL interpretation, they are regions where the phase-response does not provide a strong accumulation environment. Matter may pass through, remain diffuse, or fail to build a stable clump.

Behavior summary

3D sine intersections produce a field landscape. Amplified nodes are peaks in the landscape. Cancelled regions are valleys or boundaries. Matter does not have to be created or destroyed; it organizes more easily at stable peaks.

6 Explaining seemingly random matter clumping

A central payoff of the 3D mechanism is its explanation of apparent random clumping throughout space. In a projected image, clumps can appear irregular because the observer sees a 2D shadow of a 3D node network. The apparent randomness can be caused by projection, incomplete distance information, time evolution, and the fact that 3D interference geometry is high-order.

$$\boxed{\begin{array}{c}\text{3D phase intersections} \rightarrow \text{amplified coherence nodes} \\ \rightarrow \text{preferred baryonic accumulation} \rightarrow \text{projected clumps}\end{array}} \tag{16}$$

This does not claim that nodes create matter from nothing. It claims that existing baryonic matter preferentially organizes near stable amplified nodes. A candidate drift-diffusion expression for this hypothesis is

$$\mathbf{J}_b = -D\nabla\rho_b + \mu\rho_b\nabla C_\Phi, \tag{17}$$

$$\frac{\partial\rho_b}{\partial t} = -\nabla\cdot\mathbf{J}_b, \tag{18}$$

where D is a dispersive/diffusive coefficient and μ is an effective drift coefficient toward increasing C_Φ. Eqs. (17)–(18) are not part of the locked acceleration law. They are a possible test model for matter organization.

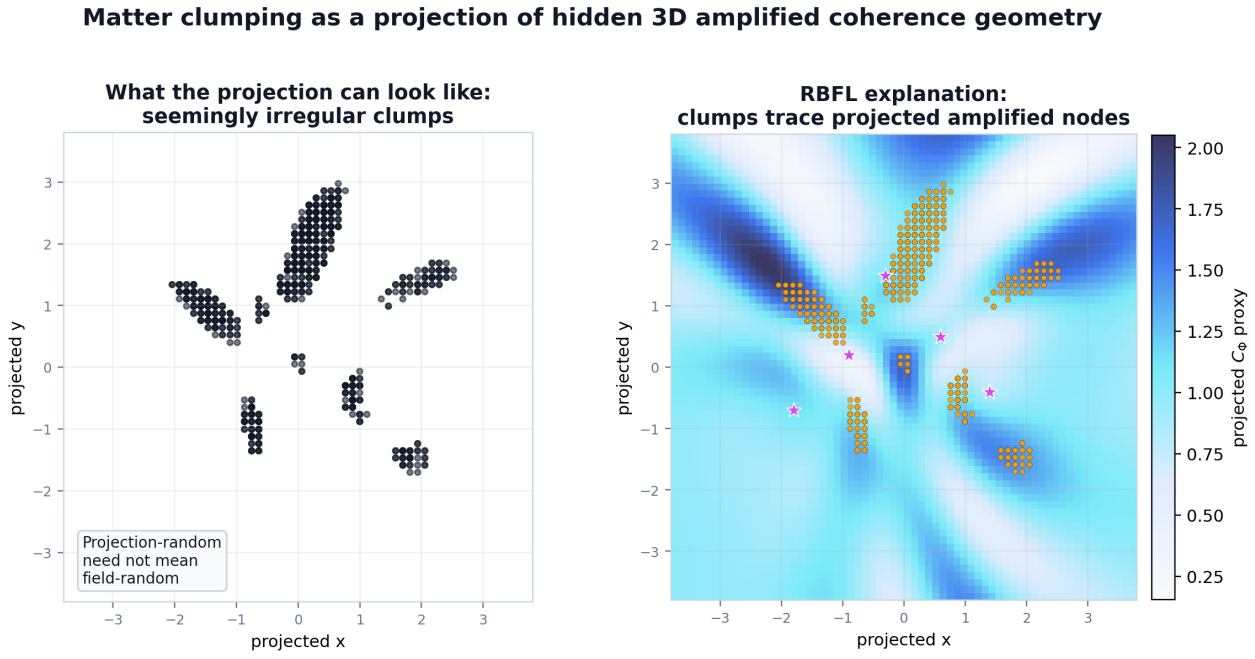

Figure 4: A projected clump pattern can look irregular. In the RBFL explanation, the same clumps may trace stable amplified nodes of the 3D field. The right panel overlays projected node intensity to show how the irregular pattern can be an ordered field projection.

Simple picture

If flour is floating in a room full of invisible sound waves, it will collect more in the loud stable spots than in the quiet spots. From one camera angle, the flour piles might look random. From the full 3D view, they trace the wave pattern.

6.1 Voids and low-density regions

The same mechanism explains low-density regions without requiring a separate rule. If constructive amplification does not occur, matter does not receive the same organizing phase environment. Therefore a void-like region can be read as a suppression zone, a non-amplified region, or a region between node networks. Observed large-scale structure is widely described as a filament-and-void network [3]; RBFL interprets such morphology as a possible projection of nested phase-node geometry.

7 Scaling from the beginning to the present 3D mechanism

The scaling story is the bridge from the empirical law to field mechanics. It can be written as a development chain.

$$\boxed{\begin{array}{c}\text{Observed scalar / radial law}\\ \Downarrow\\ \text{3D vector acceleration law}\\ \Downarrow\\ \text{Volumetric phase field } \Phi_{\text{total}}(\mathbf{r},t)\\ \Downarrow\\ \text{Sine-phase intersections}\\ \Downarrow\\ \text{Amplified coherence nodes } (C_\Phi > 1)\\ \Downarrow\\ \text{Matter clumps, filaments, void-like gaps, and scaling}\end{array}} \tag{19}$$

Sine behavior naturally introduces a wavelength scale,

$$\lambda_i = \frac{2\pi}{|\mathbf{k}_i|}. \tag{20}$$

If baryonic anchors exist across many sizes, their phase environments can also produce nodes across many effective sizes. The same rule repeats:

$$\boxed{\text{phase overlap} \rightarrow \text{constructive amplification} \rightarrow \text{stable node} \rightarrow \text{matter organization}} \tag{21}$$

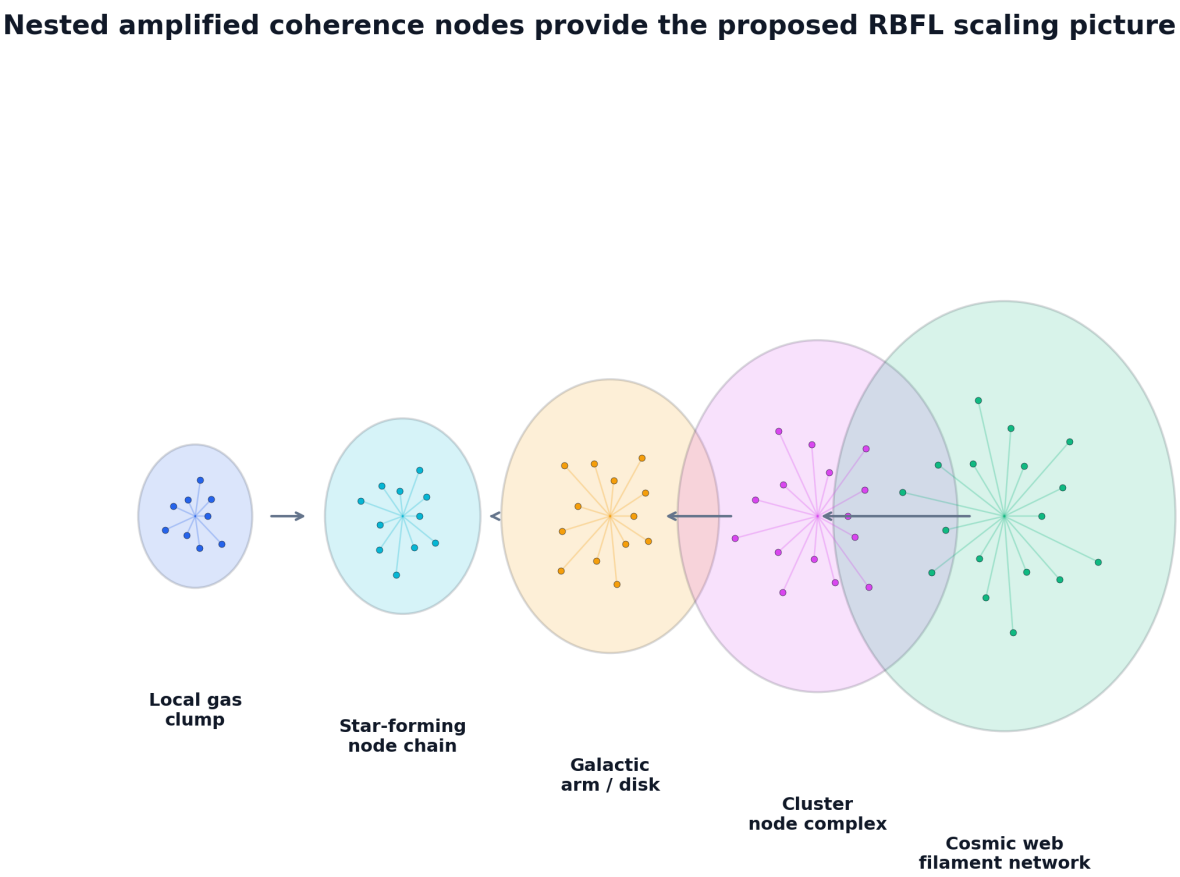

Figure 5: Proposed RBFL scaling picture. The rule is the same at different sizes, while the visible structures change. Local clumps, galactic arms, clusters, and filaments can be interpreted as nested amplified coherence-node structures.

7.1 Why this can scale without changing the law

The acceleration law does not need a new parameter for every size range because $C_\Phi(\mathbf{r}, t)$ is local. It samples the phase state at the point where the acceleration is evaluated. A small cloud, a galactic disk, a cluster, and a filament do not need different laws; they need different local values and gradients of the same 3D coherence response.

Scaling lock

RBFL scaling is interpreted as nested 3D amplified coherence-node hierarchy. The law stays the same; C_Φ carries the local phase-state information.

8 Relation to rotation curves, lensing maps, and the cosmic web

8.1 Rotation curves

Rotation curves are natural first tests because they are already reduced to radial acceleration behavior. The SPARC database, for example, provides disk-galaxy photometry and high-quality rotation curves across a broad galaxy sample [1]. In RBFL, the radial curve is a projection of the 3D field:

$$\boxed{g_{\mathrm{obs}}(R) \leftarrow \mathcal{P}_R[\mathbf{g}_{\mathrm{RBFL}}(\mathbf{r}, t)]} \tag{22}$$

where $\mathcal{P}_R$ means disk-plane extraction, radial binning, or another appropriate measurement mapping.

The scalar relation is therefore retained as a diagnostic:

$$g_{\rm obs}(R) - g_b(R) \sim C_\Phi(R)\sqrt{a_\Phi g_b(R)}. \tag{23}$$

The 3D mechanism explains why C_Φ may differ from one location or galaxy to another.

8.2 Lensing maps

A lensing map is also a projection. In RBFL notation,

$$\boxed{\kappa_{\rm obs} = \kappa_b + \kappa_\Phi, \qquad \kappa_\Phi = \mathcal{P}_{\rm lens}[\Phi_{\rm total}]} \tag{24}$$

where $\mathcal{P}_{\rm lens}$ denotes the lensing channel. This statement does not by itself solve every lensing system. It tells us how the 3D phase-field explanation should be connected to projected lensing data. Cluster lensing is a major reason dark matter is commonly invoked in standard cosmology [4]; an RBFL alternative must therefore make lensing-specific predictions, not only rotation-curve fits.

8.3 Cosmic-web morphology

The cosmic web is commonly described as a network of clusters, filaments, sheets, and voids [3]. In the sine-intersection interpretation, filaments are not merely material threads. They can be interpreted as projected chains of amplified coherence nodes. Voids are not merely empty accidents. They can be interpreted as non-amplified or suppressed regions between node networks.

$$\boxed{\text{filament} \approx \text{connected chain of } C_\Phi > 1 \text{ nodes}} \tag{25}$$

$$\boxed{\text{void-like gap} \approx \text{region lacking stable amplified } C_\Phi \text{ nodes}} \tag{26}$$

9 Defensible test program

A useful mechanism must expose itself to failure. The sine-intersection explanation is testable because it predicts structured residuals rather than arbitrary residuals.

9.1 Residual coherence estimator

Given observed and baryonic acceleration estimates, define a projected residual-coherence estimator

$$\boxed{A_\Phi^{\rm obs} = \frac{|\mathbf{g}_{\rm obs} - \mathbf{g}_b|}{\sqrt{a_\Phi |\mathbf{g}_b|}}} \tag{27}$$

which should approximate a projected form of C_Φ when the RBFL law applies.

9.2 Predictions

1. **Node correlation:** Peaks in $A_\Phi^{\rm obs}$ should correlate with reconstructed high-C_Φ 3D node locations better than with random clump placements.
2. **Suppression correlation:** Low-density gaps and void-like regions should correlate with suppressed or non-amplified regions of reconstructed C_Φ.
3. **Projection consistency:** A single 3D node reconstruction should help explain more than one projected observable, such as rotation residuals and lensing residuals, without adding separate fitted halos for each observable.
4. **Scaling consistency:** Node patterns should persist statistically across nested scales: local clumps, galactic features, group environments, cluster substructure, and filamentary structure.

5. **Phase geometry:** Residual maps should show structured interference-like geometry, not only smooth spherical halos or uncorrelated noise.

Most important falsifiable statement

If C_Φ is a physical interference response, then residual acceleration and projected clumping should map onto a reconstructible 3D phase-node geometry. If no such geometry can be reconstructed, or if the required C_Φ values are arbitrary and uncorrelated with baryonic anchors, this mechanism fails.

10 What this does and does not claim

Claim type	Position in this paper
Current RBFL 3D acceleration law	Unchanged and treated as the locked law.
2D RBFL forms	Retained as projection, slice, visualization, or diagnostic forms.
Sine-intersection behavior	Proposed mechanism for the existing coherence factor C_Φ.
Matter clumping	Proposed consequence of stable amplified nodes organizing existing baryonic matter.
Voids / gaps	Interpreted as non-amplified or suppressed regions, not necessarily as actively expelled matter.
Dark matter comparison	RBFL offers an alternative explanatory route; this paper does not claim complete replacement of all dark matter evidence.
Final equation for C_Φ	Not yet locked. Eq. (13) defines the modeling target, not a final closure.

Table 2: Defensibility boundary. The mechanism is useful because it explains the existing term, but it must not be overstated as a completed proof.

Main limitation

The sine-intersection mechanism is a mechanism-level interpretation. It becomes a complete field theory only when $\mathcal{C}[\cdots]$ is closed, calibrated, and shown to predict rotation, lensing, morphology, and clumping from the same baryonic inputs.

11 One-page visual summary

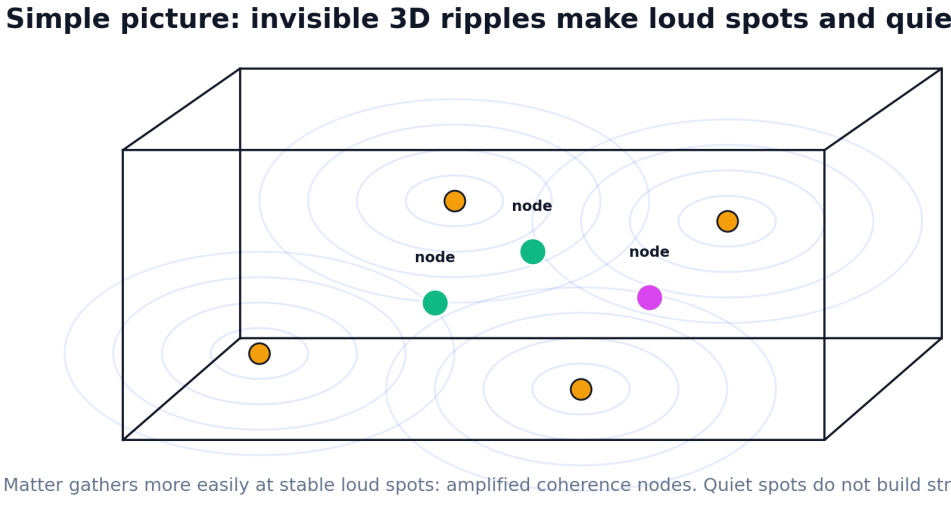

Figure 6: A child-level visualization of the full idea. Baryonic anchors behave like sources of 3D ripples. Stable loud spots are amplified coherence nodes. Matter can organize around those nodes, making clumps that look irregular from one viewing angle.

Full theory statement

RBFL treats baryonic matter as anchoring volumetric phase-compression responses inside a saturated parent field. Observed 2D data are projections of the 3D field. The existing coherence factor $C_\Phi(\mathbf{r}, t)$ is interpreted as the local response of volumetric sine-phase interference: constructive intersections produce amplified coherence nodes, while destructive intersections produce suppression or cancellation. Stable amplified nodes are candidate matter-organization sites, providing a defensible explanation for scaling, filaments, void-like gaps, and apparently random clumping without changing the current 3D RBFL acceleration law.

12 Conclusion

The 3D sine-intersection interpretation supplies the mechanism that the empirical RBFL law did not explicitly contain. The law remains

$$\mathbf{g}_{\mathrm{RBFL}} = \mathbf{g}_b + C_\Phi \sqrt{a_\Phi |\mathbf{g}_b|}\, \hat{\mathbf{g}}_b.$$

The explanatory upgrade is that $C_\Phi(\mathbf{r}, t)$ is no longer treated as an abstract fitting factor. It is interpreted as the local 3D phase-interference response of baryonic phase-compression volumes.

This creates a coherent picture:

$$\boxed{\begin{array}{l}\text{baryonic anchors} \rightarrow \text{3D phase volumes} \rightarrow \text{sine intersections} \\ \rightarrow \text{amplification/cancellation} \rightarrow C_\Phi \rightarrow \text{observed structure}\end{array}}$$

The reason 2D was used first is that the data are observed and displayed in projection. The reason 3D is required is that the field itself is volumetric. The reason sine intersections matter is that they define where coherence actually occurs: at amplification points. The reason clumping can look random is that projected clumps may be the 2D shadow of hidden 3D amplified nodes. The reason scaling can emerge is that the same phase-node rule can repeat across nested baryonic structures.

References

[1] F. Lelli, S. S. McGaugh, and J. M. Schombert, "SPARC: Mass Models for 175 Disk Galaxies with Spitzer Photometry and Accurate Rotation Curves," *The Astronomical Journal*, vol. 152, no. 6, 2016. https://arxiv.org/abs/1606.09251

[2] S. S. McGaugh, J. M. Schombert, G. D. Bothun, and W. J. G. de Blok, "The Baryonic Tully-Fisher Relation," *The Astrophysical Journal Letters*, 2000. https://arxiv.org/abs/astro-ph/0003001

[3] J. R. Bond, L. Kofman, and D. Pogosyan, "How Filaments are Woven into the Cosmic Web," *Nature*, vol. 380, pp. 603–606, 1996. https://doi.org/10.1038/380603a0

[4] D. Clowe, M. Bradac, A. H. Gonzalez, M. Markevitch, S. W. Randall, C. Jones, and D. Zaritsky, "A Direct Empirical Proof of the Existence of Dark Matter," *The Astrophysical Journal Letters*, 2006. https://arxiv.org/abs/astro-ph/0611496